nature climate change

ARTICLES

https://doi.org/10.1038/s41558-020-0824-y

Disproportionate increase in freshwater methane emissions induced by experimental warming

Yizhu Zhu[1], Kevin J. Purdy[2], Özge Eyice[1], Lidong Shen[1,3], Sarah F. Harpenslager[1,4], Gabriel Yvon-Durocher[5], Alex J. Dumbrell[6] and Mark Trimmer[1]✉

Net emissions of the potent GHG methane from ecosystems represent the balance between microbial methane production (methanogenesis) and oxidation (methanotrophy), each with different sensitivities to temperature. How this balance will be altered by long-term global warming, especially in freshwaters that are major methane sources, remains unknown. Here we show that the experimental warming of artificial ponds over 11 years drives a disproportionate increase in methanogenesis over methanotrophy that increases the warming potential of the gases they emit. The increased methane emissions far exceed temperature-based predictions, driven by shifts in the methanogen community under warming, while the methanotroph community was conserved. Our experimentally induced increase in methane emissions from artificial ponds is, in part, reflected globally as a disproportionate increase in the capacity of naturally warmer ecosystems to emit more methane. Our findings indicate that as Earth warms, natural ecosystems will emit disproportionately more methane in a positive feedback warming loop.

Methane makes a large contribution to climate change, and methane concentrations are increasing in the atmosphere[1,2]. A substantial proportion (~42% of all natural and anthropogenic sources) of methane is emitted from freshwaters (wetlands, lakes and rivers) that make a disproportionately large contribution to the global methane budget for their comparatively modest sizes[3,4]. Methane production by methanogens and its oxidation by methanotrophs drive the biological methane cycle, with the balance between the two regulating net methane emissions[5]. Methanogenesis is very sensitive to temperature[6]: for example, an increase of 10 °C would drive a 4.0-fold increase in methane production[7,8], while, in contrast, methanotrophy[9] is less sensitive to temperature[10] (being more strongly substrate limited). Due to these different physiological responses to temperature, long-term warming might alter the structure of methanogen and methanotroph communities, disturbing the balance between the two processes and ultimately increasing methane emissions[11,12].

Linking microbial community structure to ecosystem-level processes is a major theoretical challenge[13]. Therefore, measuring microbial community characteristics such as functional diversity[12,14], gene abundance[15], growth efficiency[16] and thermodynamic constraints[17] is essential to determine how microbial community structure influences ecosystem-level processes[13]. This need is particularly acute at the long-term timescale in the methane cycle, as previous investigations into the effects of warming on methanogenesis and methanotrophy were typically limited to less than one year, which may have masked the effects of any shifts in the microbial communities[12,18,19]. Key unanswered questions under the current climate warming scenarios remain: (1) does long-term warming (greater than ten years) alter the balance between methanogenesis and methanotrophy, and (2) how do any changes in the methane-related microbial communities affect net methane emissions?

We answered these questions by studying the long-term effects of warming on freshwater ecosystem-level methane cycling in 20 well-established, artificial ponds[20,21], half of which have been heated to 4 °C above the ambient temperature since September 2006. Each pond is 1.8 m wide, has a surface area of 2.5 m^2 and has approximately 50 cm of water over 10 cm of sandy sediments (Extended Data Fig. 1). After 11 years of warming, frequent measurements (three times daily) revealed an ongoing divergence in methane emissions from the surfaces of the ponds to the atmosphere between our warmed and ambient ponds (Fig. 1a and Extended Data Fig. 2). Annual methane emissions are now 2.4-fold higher under warming and far in excess of the 1.7-fold increase predicted (equation (2)) through a simple physiological response to higher temperatures alone[7,8]. Here methane emissions are approximately twofold greater at night than during the day (Extended Data Fig. 3) and throughout are dominated by diffusion (98.8%) rather than ebullition (1.2%)[22], probably because of the relatively shallow sediments in our ponds (~10 cm), but the magnitude of ebullition is similarly amplified under warming (Supplementary Fig. 1). Even though the ponds are net sinks for CO_2 (refs. [20,21]), the ratio of CH_4 to CO_2 emitted at night has also increased 1.8-fold under warming, increasing the global warming potential of the carbon gases emitted overall (Fig. 1b)[2]. These long-term observations underline the potential of climate warming to continually amplify methane emissions from freshwaters. This prediction is supported by a meta-analysis showing an increase in the capacity of wetlands, grasslands and soils to emit methane in regions with higher annual average temperatures (Fig. 1c; see Supplementary Table 1 for the sites included) and by observations of increased methane emissions, driven by a fundamental change in the ecosystem, along a natural gradient of thawing permafrost[23]. These observations clearly show that the methane cycle does not respond to warming through a simple physiological response, but rather responds to shifts in the structure and/or activity of the overall methane-related microbial community. This more complex response to warming will affect how we predict changes in methane emissions under climate warming scenarios.

[1]School of Biological and Chemical Sciences, Queen Mary University of London, London, UK. [2]School of Life Sciences, University of Warwick, Coventry, UK. [3]Institute of Ecology, School of Applied Meteorology, Nanjing University of Information Science and Technology, Nanjing, China. [4]Department of Ecosystem Research, Leibniz Institute of Freshwater Ecology and Inland Fisheries (IGB), Berlin, Germany. [5]Environment and Sustainability Institute, University of Exeter, Penryn Campus, Penryn, UK. [6]School of Life Sciences, University of Essex, Colchester, UK. ✉e-mail: m.trimmer@qmul.ac.uk

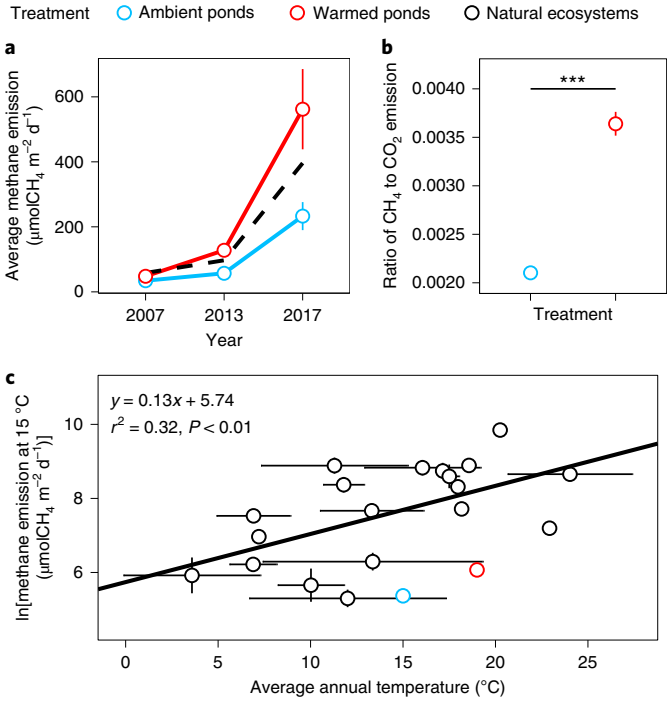

Fig. 1 | Ongoing divergence in methane emissions from the surfaces of our ponds mirrors natural warming. a, Emissions from our warmed and ambient ponds in 2007 (ref. [35]), 2013 (ref. [20]) and 2017 ($n = 3{,}553$, this study) have continued to diverge beyond that predicted for their 4 °C difference in temperature (black dashed line, equation (2) and Methods). **b**, Ratio of CH_4 to CO_2 emitted at night (measured in 2017, $n = 4{,}884$, Methods) is 1.8-fold higher with warming (*t*-test, $^{***}P < 0.001$). **c**, Our disproportionate increase in methane emissions in 2017 (**a**) maps onto a trend of increasing capacity of naturally warmer ecosystems, including wetlands, croplands and forests (Methods), to emit more methane—standardized to 15 °C. The vertical and horizontal lines represent the 95% confidence intervals (CIs).

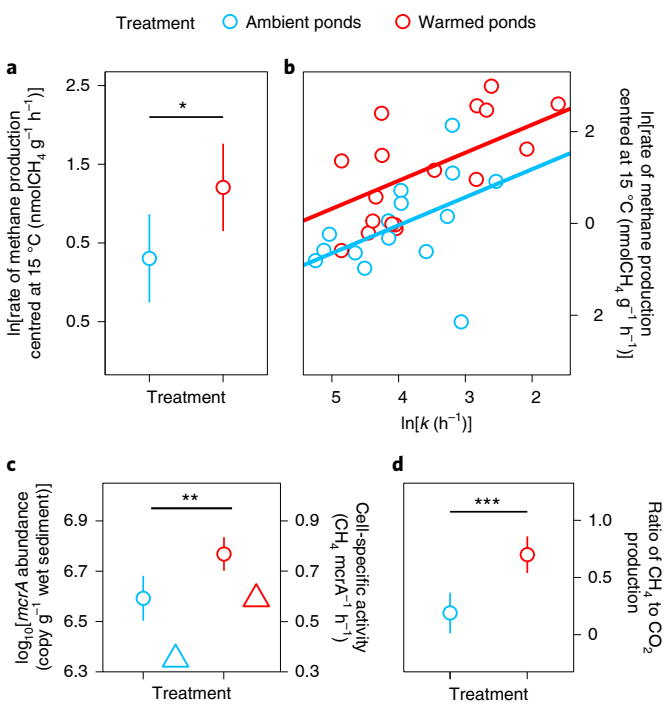

Fig. 2 | Long-term warming increases methane production over methanogen abundance. a, In the laboratory ($n = 238$, without additional substrates), warmed sediments produced more methane than ambient sediments, standardized to 15 °C. **b**, Production increased equally ($n = 32$, $P = 0.4$) with *k* in both treatments, but warming stepped up the fraction of carbon turned over to methane ($P < 0.01$). **c**, Warming increased methanogen abundance (circles) and methanogen efficiency (activity, triangles, $n = 79$). **d**, Ratio of CH_4 to CO_2 produced by warmed sediments was about threefold higher than that produced by ambient sediments ($n = 218$). As ~95% of CH_4 is oxidized to CO_2 before emission from the ponds, the laboratory ratio of CH_4 to CO_2 is higher (Fig. 1b). The vertical lines represent the 95% CIs. $^{*}P < 0.05$; $^{**}P < 0.01$; $^{***}P < 0.001$.

To rationalize the disproportionate increases in both CH_4 emissions and ratio of CH_4 to CO_2 after 11 years of warming, we measured the methane production capacity of the pond sediments at the same temperature (15 °C) in the laboratory in controlled microcosms. Warmed pond sediments produced 2.5-fold more methane than their ambient controls (post hoc pairwise comparisons, $P < 0.05$, Fig. 2a,b) for the same quality of carbon (carbon turnover (*k*), *t*-test, $P = 0.053$; see also C to N ratio in Supplementary Table 2). The potential of sediments to produce methane increased equally in both the warmed and ambient ponds as carbon quality also increased (Fig. 2b, $P = 0.4$). Warming has, however, stepped up the fraction of carbon turned over to methane because methanogens are now 1.5-fold more abundant in the warmed ponds (quantitative PCR (qPCR) of the *mcrA* gene, Fig. 2c, circles, *t*-test, $P < 0.05$) and, importantly, methanogens in the long-term warmed ponds seemed to be ~60% more efficient at making methane (Fig. 2c, triangles). This increase in methanogen efficiency explains the disproportionate increase in methane emissions (Fig. 1a) and, by increasing the ratio of CH_4 to CO_2 produced in the sediment by threefold (*t*-test, $P < 0.001$, Fig. 2d), also accounts for the increased ratio of CH_4 to CO_2 emitted to the atmosphere at night (Fig. 1b). These increases are, however, hard to rationalize without a fundamental change to the structure of the methanogen community.

In freshwater sediments, methane is produced predominantly by acetoclastic and hydrogenotrophic methanogenesis[24]. Theoretically, these two types of methanogenesis have stoichiometric equivalence, and complete glucose degradation should produce CH_4 and CO_2 in a 1:1 ratio, with 33% CH_4 from hydrogenotrophy and 67% CH_4 from acetoclastic methanogenesis (refs. [24,25] and Supplementary Discussion). Just as in our pond sediments (Fig. 2d), however, this idealized 1:1 ratio is seldom found, with deviations from 1:1 being ascribed to differences in organic matter oxidation state, pH or organic matter quality[26–28] that do not apply to our ponds. We would argue instead that the proportion of available H_2 flowing to methane increases under warming[17,27] (Supplementary Discussion) and that the increase in both methanogen efficiency and CH_4-to-CO_2 ratios (Figs. 1b and 2c,d) suggested a shift towards hydrogenotrophic methanogenesis with long-term warming. We tested this hypothesis by analysing the methanogen communities and identified significant shifts in two dominant hydrogenotrophic genera between the warmed and ambient ponds (Fig. 3a,b and Supplementary Tables 3 and 4) but no significant changes in any other methanogens (for example, acetoclastic genera). Specifically, the relative abundance of *Methanobacterium* increased significantly from 8.5% to 13.2% of the methanogen community, whereas *Methanospirillum* decreased from 31.3% to 22.7% between the ambient and warmed ponds, respectively (adjusted $P < 0.01$, Fig. 3b). After 11 years of warming, the methanogen diversity was conserved (Supplementary Fig. 2), but marginal changes in the relative abundance of *Methanobacterium* and *Methanospirillum* and other minor changes within the community (with four hydrogenotrophic genera increasing in relative abundance and two new genera appearing in the warmed ponds;

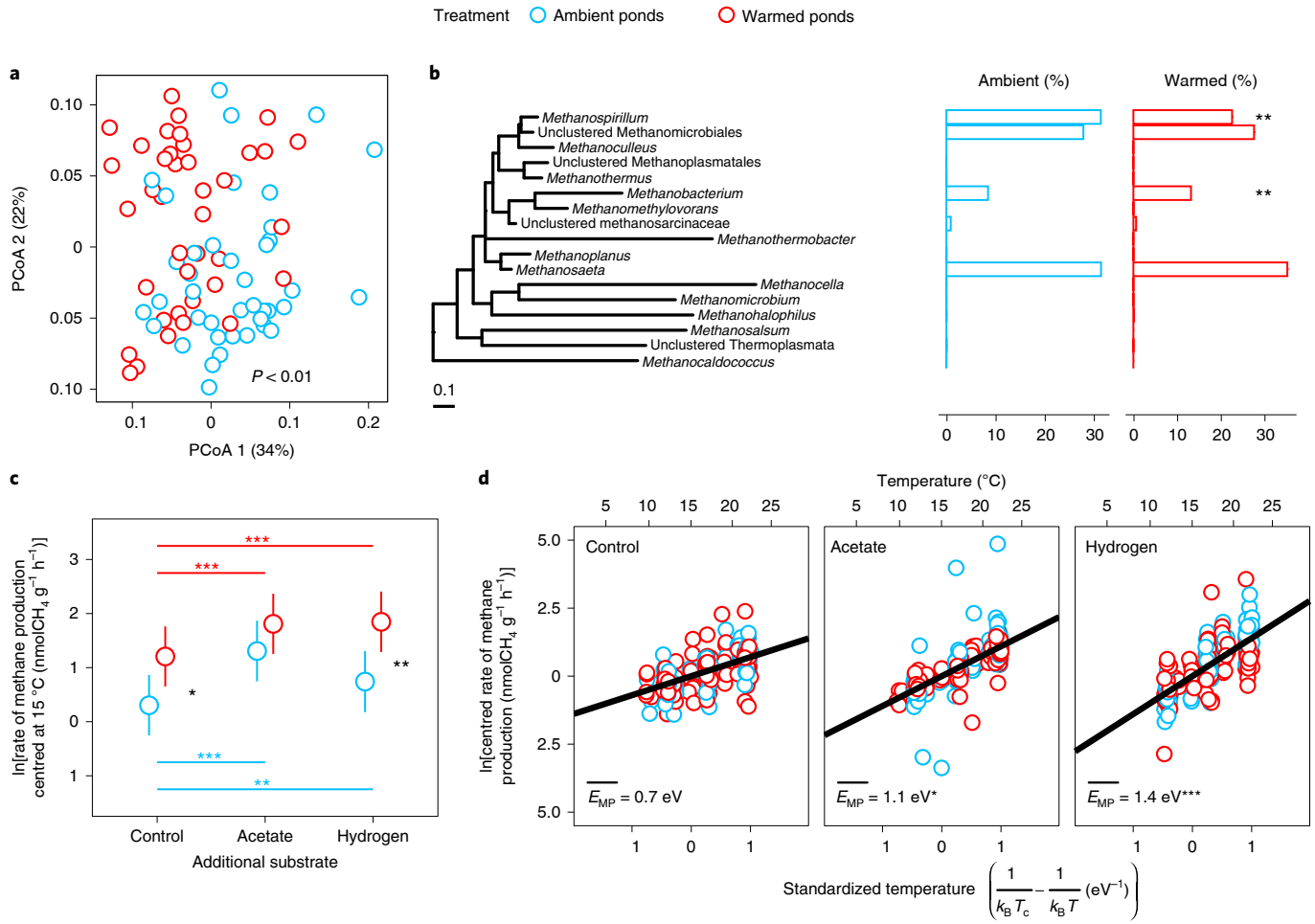

Fig. 3 | Long-term warming provides a mechanism to selectively alter the methanogen community. a,**b**, Significant shifts in the methanogen community between ambient and warmed ponds ($n = 79$, principal coordinate analysis (PCoA) at the genus level; see Methods) (**a**) were due to significant shifts in the relative abundances of two hydrogenotrophic genera (*Methanospirillum* and *Methanobacterium*) (**b**). In **b**, the relative changes in abundance (%), indicated by horizontal bars in the bar chart to the right, align with their respective genera in the tree on the left. **c**, Hydrogen-stimulated methanogenesis in the warmed pond sediments above that for acetate ($n = 662$). The vertical lines represent the 95% CIs. Statistical significance is compared with the controls and between the warmed and ambient ponds by asterisks between the means (*$P < 0.05$; **$P < 0.01$; ***$P < 0.001$). **d**, Hydrogenotrophy is more sensitive to temperature, and warming makes hydrogenotrophy more favourable to selectively alter the methanogen community.

Supplementary Table 4) seemed to be linked to the increased contribution from hydrogenotrophic methanogenesis—increasing methane production and the ratio of CH_4 to CO_2 emitted. Other ecosystems, such as thawing peat permafrost, also show increased methane emissions on warming[23], but these emissions are linked to fundamental successional changes in the methanogen community that match successional changes in the ecosystem. Yet, our freshwater ponds show that subtle shifts in the methanogen community can produce substantial changes in the methane emissions of these ecosystems under warming, suggesting that natural freshwater systems are likely to be capable of responding in a similar manner (Fig. 1c and refs. [7,27]).

We performed further incubations with the addition of hydrogen and acetate (Fig. 3c) to identify a mechanism for these changes in the methanogen community and measured a disproportionate increase in methane production with hydrogen in the warmed pond sediments (Fig. 3c). Further short-term temperature manipulations also clearly showed that hydrogenotrophic methanogenesis was the most sensitive to temperature, with an apparent activation energy of 1.40 eV for H_2 compared with 0.7 eV for the controls (post hoc pairwise comparisons, $P < 0.001$, Fig. 3d). Thus, warming makes hydrogenotrophic methanogenesis more favourable, providing a mechanism to drive the shift towards a more hydrogenotrophic methanogenesis due to warming.

Short-term (less than three months) experiments in wetlands have shown that the relative contribution of hydrogenotrophic methanogenesis decreases at lower temperatures[17,27,29–31]. Conversely, hydrogenotrophy dominates in warmer freshwater environments, and a community meta-analysis identified strong selection for hydrogenotrophic methanogens in warm environments[32–34]. Here we demonstrate experimentally that the long-term warming of a freshwater community favours hydrogenotrophic over acetoclastic methanogenesis, altering both the efficiency and structure of the methanogen community to increase the ratio of produced and emitted CH_4 to CO_2 (Figs. 1b, 2d and 3a,b). Our observations reflect subtle changes in the structural and functional ecology of shallow ponds in stark contrast to the major changes seen in hydrology, vegetation, organic matter quality and pH along a natural gradient of thawing permafrost[23], where increases in methane emissions run alongside major alterations to the methanogen community. Furthermore, the predictable physiological increase in methane emissions seen after one year of experimental warming in peatland soils[19] mirrors what

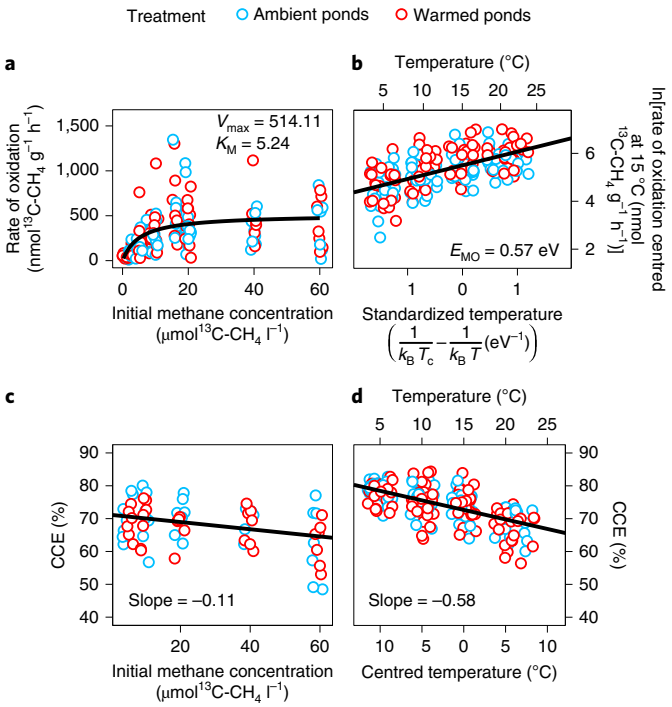

Fig. 4 | Methane oxidation is conserved and the growth of methanotrophy is impaired under warming. a, Strong physiological response in methane oxidation to higher methane in the laboratory, with a comparable capacity in warmed and ambient pond sediments ($n = 158$, $P > 0.05$ for V_{max}, the maximum rate, and K_M, the concentration of methane at half V_{max}). **b**, A similarly conserved response to temperature ($n = 192$, $P = 0.068$). **c**,**d**, Methanotrophic growth efficiency (that is, CCE) was impaired at higher methane concentrations ($n = 69$, $P < 0.01$) (**c**) and at higher temperatures ($n = 191$, $P < 0.01$) (**d**)—that is, the conditions induced by warming in the ponds. Under substrate limitation and impaired growth, the methanotroph community was conserved and lacked the potential to reach the required abundance to balance the increase in methane production under warming.

we first observed in our ponds[35]. If ongoing warming sets peat on a similar trajectory, as our meta-analysis suggests, then we would predict disproportionate increases in methane emissions from peatlands too.

The balance between methane production and its oxidation controls the net emission of methane. We used similar laboratory microcosm incubations to those described above to investigate whether long-term warming enhanced methane oxidation to the same magnitude as methane production. In contrast to methane production, however, we found the sediments' capacity to oxidize methane to be the same in both our warmed and ambient ponds (likelihood ratio test (LRT), $P = 0.93$, Fig. 4a). The methanotrophs did have a strong kinetic potential to oxidize more methane, and warming-induced increases in methane concentrations in the ponds (2.1-fold, Supplementary Table 2) were reflected in increased methane oxidation activity in the laboratory (1.9-fold; see equation (7) for the Michaelis–Menten model). Similarly, while the temperature sensitivity of methane oxidation—in the laboratory—was the same in both warmed and ambient pond sediments (LRT, $P = 0.24$, Fig. 4b), the 4 °C of warming in situ would increase methane oxidation activity too (that is, a 1.4-fold increase with the common activation energy of 0.57 eV in equation (2)). Altogether, higher methane concentrations and the 4 °C of warming would increase the methane oxidation capacity of the warmed ponds 2.6-fold (Supplementary Table 2). Furthermore, as methanotrophic activity is confined to a thin, oxic zone at the sediment surface[36], which was ~40% shallower in the warmed ponds (Supplementary Fig. 3), there would have been an oxygen effect too. Combined, the methane kinetic, temperature and oxygen-penetration effects (1.9-, 1.4- and 1.4- fold, respectively) would drive 3.6-fold greater methane oxidation activity in the warmed ponds (see Supplementary Table 2 and further discussion therein) that would ultimately attenuate ~95% of the extra methane production under warming but not the 98% required to prevent increased methane emissions. This poses the question: why might methanotrophs not be able to keep up with methanogens under warming?

Methanotroph abundance did increase in the warmed ponds, but not enough (2.45-fold versus 2.67-fold required; see Supplementary Table 2) to offset the greater warming-induced methane production. As a proxy for their growth efficiency[16], we measured the fraction of methane assimilated into methanotroph biomass (carbon conversion efficiency (CCE)) in the laboratory. Accordingly, methanotroph CCE was indistinguishable between the warmed and ambient sediments; however, methanotroph CCE was suppressed at both higher methane concentrations and higher temperatures (Fig. 4c,d)—that is, the exact conditions induced by warming. In the ponds, therefore, the warmed methanotrophs would assimilate a smaller fraction of their metabolized methane, grow less efficiently and thus lack the potential to reach the required abundance to balance greater methane production. Whereas we cannot predict the increase in methane production from a simple physiological response to warming, we could determine just such a simple physiological response for methane oxidation. In contrast to warming-induced change in the methanogen community, the methanotroph community was conserved (Supplementary Fig. 4 and Supplementary Table 3); it is noticeable, however, that 11 of the 16 detected operational taxonomic units (OTUs) had lower relative abundances (with two genera being undetected) in the warmed ponds (Supplementary Table 5). We propose that whereas warming makes hydrogenotrophic methanogenesis more favourable (thus changing the methanogen community), there is no similar mechanism to favourably alter the methanotroph community.

Our long-term warming experiment provides a mechanistic understanding of a potential positive feedback warming loop in the freshwater methane cycle. In particular, warming increases the efficiency of methanogenesis and preferentially alters hydrogenotrophy while limiting the capacity of methanotrophs to consume methane by impairing their growth, which together increase the global warming potential of the carbon gases emitted. These emergent properties increase methane emissions far beyond a simple physiological increase in response to warming alone, and what we have witnessed under experimental warming is, in part, borne out at the global scale as a disproportionate increase in the capacity of a variety of naturally warmer ecosystems (for example, wetlands, croplands, forests and grasslands; see Methods) to emit methane. Together, our findings strongly indicate that as Earth continues to warm, natural ecosystems will emit disproportionately more methane to the atmosphere in a positive feedback warming loop (Fig. 5).

Online content

Any methods, additional references, Nature Research reporting summaries, source data, extended data, supplementary information, acknowledgements, peer review information; details of author contributions and competing interests; and statements of data and code availability are available at https://doi.org/10.1038/s41558-020-0824-y.

Received: 7 December 2019; Accepted: 15 May 2020;
Published online: 29 June 2020

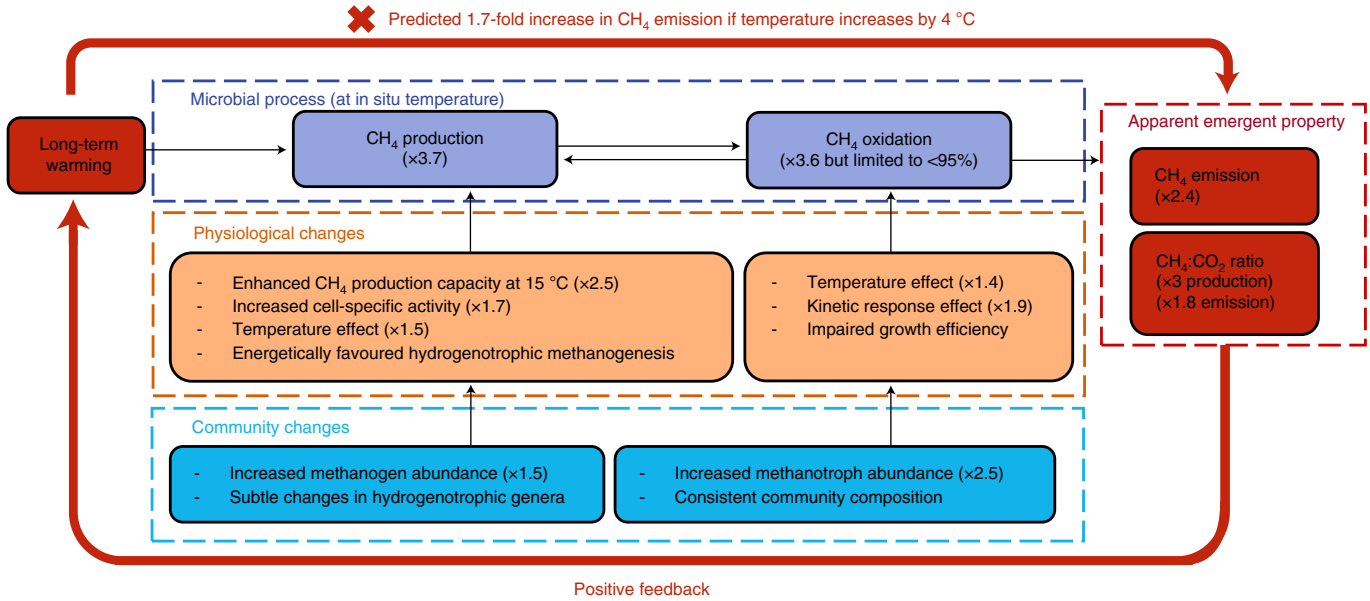

Fig. 5 | Positive climate warming feedback loop revealed by our long-term experiment. Methane emissions cannot be predicted by temperature alone, and both the magnitude of emission and the ratio of CH_4 to CO_2 increase as apparent emergent properties of changes in the overall methane cycle (outer, red arrow). Long-term warming favours hydrogenotrophic methanogenesis, providing a mechanism to alter both the efficiency (middle, orange rectangles) and structure of the methanogen community (bottom, cyan rectangles). In contrast, there is no similar mechanism to alter the methanotroph community, and physiological responses dominate. Methane oxidation cannot offset the extra methane production under warming (top, blue rectangles), and a positive feedback loop in the methane cycle develops through global warming.

References

1. Nisbet, E. G., Dlugokencky, E. J. & Bousquet, P. Methane on the rise—again. *Science* **343**, 493–495 (2014).
2. Balcombe, P., Speirs, J. F., Brandon, N. P. & Hawkes, A. D. Methane emissions: choosing the right climate metric and time horizon. *Environ. Sci. Process. Impacts* **20**, 1323–1339 (2018).
3. Holgerson, M. A. & Raymond, P. A. Large contribution to inland water CO_2 and CH_4 emissions from very small ponds. *Nat. Geosci.* **9**, 222–226 (2016).
4. Saunois, M. et al. The global methane budget 2000–2012. *Earth Syst. Sci. Data* **8**, 697–751 (2016).
5. Bridgham, S. D., Cadillo-Quiroz, H., Keller, J. K. & Zhuang, Q. Methane emissions from wetlands: biogeochemical, microbial, and modeling perspectives from local to global scales. *Glob. Change Biol.* **19**, 1325–1346 (2013).
6. Gudasz, C. et al. Temperature-controlled organic carbon mineralization in lake sediments. *Nature* **466**, 478–481 (2010).
7. Yvon-Durocher, G. et al. Methane fluxes show consistent temperature dependence across microbial to ecosystem scales. *Nature* **507**, 488–491 (2014).
8. Allen, A. P., Gillooly, J. F. & Brown, J. H. Linking the global carbon cycle to individual metabolism. *Funct. Ecol.* **19**, 202–213 (2005).
9. Hanson, R. S. & Hanson, T. E. Methanotrophic bacteria. *Microbiol. Rev.* **60**, 439–471 (1996).
10. Shelley, F., Abdullahi, F., Grey, J. & Trimmer, M. Microbial methane cycling in the bed of a chalk river: oxidation has the potential to match methanogenesis enhanced by warming. *Freshw. Biol.* **60**, 150–160 (2015).
11. Mohanty, S. R., Bodelier, P. L. E. & Conrad, R. Effect of temperature on composition of the methanotrophic community in rice field and forest soil. *FEMS Microbiol. Ecol.* **62**, 24–31 (2007).
12. Høj, L., Olsen, R. A. & Torsvik, V. L. Effects of temperature on the diversity and community structure of known methanogenic groups and other archaea in high Arctic peat. *ISME J.* **2**, 37–48 (2008).
13. Hall, E. K. et al. Understanding how microbiomes influence the systems they inhabit. *Nat. Microbiol.* **3**, 977–982 (2018).
14. Ho, A., Lüke, C. & Frenzel, P. Recovery of methanotrophs from disturbance: population dynamics, evenness and functioning. *ISME J.* **5**, 750–758 (2011).
15. Rocca, J. D. et al. Relationships between protein-encoding gene abundance and corresponding process are commonly assumed yet rarely observed. *ISME J.* **9**, 1693–1699 (2015).
16. Trimmer, M. et al. Riverbed methanotrophy sustained by high carbon conversion efficiency. *ISME J.* **9**, 2304–2314 (2015).
17. Fey, A. & Conrad, R. Effect of temperature on carbon and electron flow and on the archaeal community in methanogenic rice field soil. *Appl. Environ. Microbiol.* **66**, 4790–4797 (2000).
18. Ho, A. & Frenzel, P. Heat stress and methane-oxidizing bacteria: effects on activity and population dynamics. *Soil Biol. Biochem.* **50**, 22–25 (2012).
19. Wilson, R. M. et al. Stability of peatland carbon to rising temperatures. *Nat. Commun.* **7**, 13723 (2016).
20. Yvon-Durocher, G., Hulatt, C. J., Woodward, G. & Trimmer, M. Long-term warming amplifies shifts in the carbon cycle of experimental ponds. *Nat. Clim. Change* **7**, 209–213 (2017).
21. Yvon-Durocher, G. et al. Five years of experimental warming increases the biodiversity and productivity of phytoplankton. *PLoS Biol.* **13**, e1002324 (2015).
22. Davidson, T. A. et al. Synergy between nutrients and warming enhances methane ebullition from experimental lakes. *Nat. Clim. Change* **8**, 156–160 (2018).
23. McCalley, C. K. et al. Methane dynamics regulated by microbial community response to permafrost thaw. *Nature* **514**, 478–481 (2014).
24. Conrad, R. Contribution of hydrogen to methane production and control of hydrogen concentrations in methanogenic soils and sediments. *FEMS Microbiol. Ecol.* **28**, 193–202 (1999).
25. Wilson, R. M. et al. Hydrogenation of organic matter as a terminal electron sink sustains high CO_2:CH_4 production ratios during anaerobic decomposition. *Org. Geochem.* **112**, 22–32 (2017).
26. Hodgkins, S. B. et al. Changes in peat chemistry associated with permafrost thaw increase greenhouse gas production. *Proc. Natl Acad. Sci. USA* **111**, 5819–5824 (2014).
27. Glissmann, K., Chin, K. J., Casper, P. & Conrad, R. Methanogenic pathway and archaeal community structure in the sediment of eutrophic Lake Dagow: effect of temperature. *Microb. Ecol.* **48**, 389–399 (2004).
28. Inglett, K. S., Inglett, P. W., Reddy, K. R. & Osborne, T. Z. Temperature sensitivity of greenhouse gas production in wetland soils of different vegetation. *Biogeochemistry* **108**, 77–90 (2012).
29. Conrad, R., Klose, M. & Noll, M. Functional and structural response of the methanogenic microbial community in rice field soil to temperature change. *Environ. Microbiol.* **11**, 1844–1853 (2009).
30. Metje, M. & Frenzel, P. Methanogenesis and methanogenic pathways in a peat from subarctic permafrost. *Environ. Microbiol.* **9**, 954–964 (2007).
31. Nozhevnikova, A. N. et al. Influence of temperature and high acetate concentrations on methanogenesis in lake sediment slurries. *FEMS Microbiol. Ecol.* **62**, 336–344 (2007).
32. Wen, X. et al. Global biogeographic analysis of methanogenic archaea identifies community-shaping environmental factors of natural environments. *Front. Microbiol.* **8**, 1339 (2017).

33. Conrad, R. et al. Stable carbon isotope discrimination and microbiology of methane formation in tropical anoxic lake sediments. *Biogeosciences* **8**, 795–814 (2011).
34. Kotsyurbenko, O. R. Trophic interactions in the methanogenic microbial community of low-temperature terrestrial ecosystems. *FEMS Microbiol. Ecol.* **53**, 3–13 (2005).
35. Yvon-Durocher, G., Montoya, J. M., Woodward, G., Jones, J. I. & Trimmer, M. Warming increases the proportion of primary production emitted as methane from freshwater mesocosms. *Glob. Change Biol.* **17**, 1225–1234 (2011).
36. Reim, A., Lüke, C., Krause, S., Pratscher, J. & Frenzel, P. One millimetre makes the difference: high-resolution analysis of methane-oxidizing bacteria and their specific activity at the oxic–anoxic interface in a flooded paddy soil. *ISME J.* **6**, 2128–2139 (2012).

Methods

Mesocosm pond facility. Twenty artificial ponds were installed in 2005 at the Freshwater Biological Association's River Laboratory in Dorset, UK (2°10′ W, 50°30′ N). The ponds (1.8 m in diameter and 2.5 m^2) hold 1 m^3 of water (50 cm deep), have a 6–10 cm layer of fine sand sediment and were seeded with local communities of macroinvertebrates and plants to mimic shallow lakes[20,21,35]. The ponds are arranged in a randomized-block design, with half of the ponds being warmed by 4 °C above ambient temperatures since 2006 (Extended Data Fig. 1).

Methane and carbon dioxide emissions from the surfaces of the ponds. Methane and carbon dioxide emissions from the surfaces of the ponds were measured about three times per day from February 2017 to February 2018 using a combination of an Ultra-Portable Greenhouse Gas Analyzer (915-0011, LGR, Los Gatos Research), a Multi-port Inlet Unit (MIU, LGR), 14 dynamic chambers (internal dimater (Ø): 20 cm; volume: 0.43 l; model 8100-101, LI-COR) and a customized Campbell control unit (CCU) (Extended Data Fig. 1). Each dynamic chamber floats on a ring permanently fixed at the centre of seven of the ten warmed and seven of the ten ambient ponds and are connected to 1 to 14 of the inlet ports on the MIU, which is connected to the inlet port of the LGR that pumps air at ~3 l min^{-1}. As the LGR cannot operate the dynamic chambers directly, the CCU triggers them sequentially after receiving a signal from the LGR. Each chamber remains open until triggered to close for a 30 min sampling period, at which point the MIU switches to the closing chamber to direct gas to the LGR. A complete cycle takes ~8 h, including background atmospheric methane. Between each chamber the CCU synchronizes the MIU and LGR to avoid any drift in the sequence. The data were acquired at 1 Hz, and methane or carbon dioxide emissions were calculated at steady state by[37]:

$$F = \frac{(C_{\text{obseravtion}} - C_{\text{background}})}{S_{\text{area}}} \times \frac{V_{\text{aeration}}}{\mathrm{d}t} \quad (1)$$

where F is the emission (μmol m^{-2} h^{-1}), $C_{\text{observation}}$ is the concentration of methane or carbon dioxide (μmol l^{-1}) at steady state (estimated by averaging the concentrations), $C_{\text{background}}$ is their respective atmospheric concentrations (μmol l^{-1}), V_{aeration}/dt is the volume of air flowing through a chamber per hour and S_{area} is the surface area of the dynamic chamber (0.031 m^2). We also needed to characterize ebullition events that lead to rapid increases in methane concentrations over short periods of time and bias our emission estimates (see Supplementary Fig. 6 for examples). An ebullition event was identified as a consistent increase in methane concentrations over 5 s at a rate greater than 50 ppb per second, to a maximum concentration, or consistent decrease for 5 s, at a rate greater than 10 ppb per second, after the post-ebullition maxima. We acknowledge that these criteria also identify other non-steady flux events besides ebullition, and we subsequently distinguished these events from ebullition if their maximum methane concentration was lower than atmospheric methane (that is, noise). Of the 16,504 total chamber measurements, 198 (1.2%) were identified as ebullition, and 7 (0.04%) were identified as other non-steady-state events. Both ebullition and other non-steady flux events were excluded from further calculations.

Predicting methane emissions, production and oxidation from their apparent activation energies. Activation energy is a measure of temperature sensitivity[7,8]. For example, the common activation energy (E_a) for methane emission of 0.96 eV predicts a 1.70-fold increase in emissions under our 4 °C warming scenario according to:

$$\frac{R(T_{\text{W}})}{R(T_{\text{A}})} = e^{\frac{E_a}{k_B T_{\text{W}}} - \frac{E_a}{k_B T_{\text{A}}}} \quad (2)$$

where $R(T)$ is the metabolic rate (for example, methane emission and similarly for production or oxidation), T_{W} and T_{A} are the mean annual temperatures of the warmed and ambient ponds (288.15 and 292.15 K, respectively) and k_{B} is the Boltzmann constant (8.62×10^{-6} eV K^{-1}).

Potential methane production with temperature and additional substrates. The pond setup provided ten independent replicates for the warmed and ambient pond treatments (Extended Data Fig. 1). Three cores of intact sediment (typically 6 cm to 10 cm depth) were collected by hand using small Perspex corers (Ø 34 mm × 300 mm) and butyl stoppers, every month from January 2016 to December 2016 (except for July) from three to five warmed and ambient ponds (four on average), selected randomly. The intact cores of sediment were stored in zip-lock bags and kept cool with freezer blocks for transport back to the laboratory (<4 h) and then kept in the dark at 4 °C.

Subsamples (~3 g) of the bottom sediment layers (below 4 cm) from the same pond were homogenized; thus, no further pseudo-replication was included within each pond. These subsamples were aliquoted into gas-tight vials (12 ml, Labco, Exetainer) inside an anoxic glove box (CV204, Belle Technologies) filled with oxygen-free nitrogen (OFN, BOC). The capacity and temperature sensitivity of methanogenic potentials with either additional acetate or hydrogen as substrates were quantified. For acetate, pond water (3.6 ml) and acetate stock solutions (0.4 ml, 100 mM, Sigma-Aldrich, for molecular biology) were flushed with OFN for 10 min and then added to each vial to create final concentrations of 10 mM, and the vials were sealed. For hydrogen, 4 ml of OFN-flushed pond water were added to each vial, and the vials were sealed and injected with 1 ml of pure hydrogen (H_2, research grade, BOC, Industrial Gases) to create a ~17% H_2 headspace (v/v). A further set of vials were left unamended as controls (see Supplementary Table 7 for the sample size). All the prepared vials were then incubated in separate batches at approximately 12 °C, 17 °C, 22 °C and 26 °C (the precise temperature could vary by 2 °C between months) for up to four days and shaken by hand twice per day. The production of methane and carbon dioxide was quantified every 24 h using a gas chromatogram fitted with a hot-nickel methanizer and flame-ionization detector (Agilent Technology UK Ltd.), as before[16,38].

Methane oxidation and its CCE. Three sediment cores were collected from eight warmed and eight ambient ponds using truncated syringes (25 ml) in May, June and July 2017 to measure the temperature sensitivity and capacity of methane oxidation. In December 2018, three sediment cores were collected from the same ponds to measure the kinetic concentration effect on methane oxidation rates. The sediment cores were kept cool and transported as described above.

The top 2 cm of sediment from each pond was homogenized and transferred into gas-tight vials (12 ml, Labco, Exetainer) along with the overlying pond water (4 ml). The vials were then sealed to leave a headspace of air. We quantified the effect of long-term warming on both the temperature and kinetic response of methane oxidation. For temperature, we enriched the vials with 200 μl of ^{13}C-CH_4 (99% atom) to 40 μmol l^{-1} in the water phase. The control vials were set up without ^{13}C-CH_4 enrichment, and all vials were incubated with gentle shaking (130 rpm) at 5 °C, 10 °C, 15 °C and 22 °C to mix the ^{13}C-CH_4 throughout the slurry. The methane concentrations described here are higher than in our ponds to enable short incubations (~22 h) at the different temperatures and avoid being confounded by substrate limitation. For the kinetic response, the vials were enriched with ^{13}C-CH_4 to 1 to 60 μmol l^{-1} in the water phase, and the vials were incubated as above at 22 °C. Vials below 15 μmol l^{-1} ^{13}C-CH_4 were incubated for <12 h, and those at higher initial concentrations were incubated for ~20 h; the experiments were then fixed by injecting 200 μl $ZnCl_2$ (50% w/v).

The CCE of methanotrophy was estimated using the fraction of ^{13}C-CH_4 recovered as ^{13}C-inorganic carbon as per ref. [16]: $1 - \frac{\Delta^{13}\text{C–inorganic}}{\Delta^{13}\text{C–CH}_4}$ where Δ represents the production of ^{13}C-inorganic or the consumption of ^{13}C-CH_4.

Oxygen profile measurements. Dissolved oxygen concentrations in the water overlying the sediments were measured from October 2015 to October 2016 in seven warmed and seven ambient ponds, using oxygen sensors (miniDOT oxygen logger, PME) at 10 min intervals. The penetration of oxygen into the sediments was measured in April 2016, at a resolution of 100 μm, as described in ref. [39].

Statistical analysis. All statistical analyses were performed in R v.3.2.5 (ref. [40]).

Annual methane emissions. The rates of methane emission were natural-log-transformed and fitted into generalized additive mixed-effect models to characterize the average annual emission patterns for the warmed or ambient ponds as a fixed effect, as before[20]. The annual rates of methane emissions were calculated using the parameter estimates from the best generalized additive mixed-effect model (Supplementary Table 6) and extrapolated to a year by multiplying by 365.

Ratio of CH_4 to CO_2 emitted from the surfaces of the ponds and produced in anoxic sediments. Our artificial ponds are net sinks for CO_2 (refs. [20,21]). To illustrate the connection between our sediment potential measurements for CH_4 and CO_2 production in the laboratory, we compared them with the emission ratio for CH_4 and CO_2 from the ponds at night when they emitted both CH_4 and CO_2. Before statistical analysis, the ratio data above the 95th percentiles for each treatment were characterized as outliers and removed. The significance of the main treatment effect (that is, warmed or ambient ponds) was then determined using the t-statistic.

Meta-analysis on methane emission capacity across a natural temperature gradient. There were 491 datasets available on the AmeriFlux (http://ameriflux.lbl.gov/) and EuroFlux networks (http://www.europe-fluxdata.eu/) (Supplementary Table 1). Of those, only 26 were for methane and air temperature, and only 19 of the available sites covered at least six months of the year and demonstrated a good relationship ($P < 0.05$) between methane emission and air temperature. Half-hour aggregated eddy-covariance data were downloaded for these 19 sites, which are wetlands (68%), forests, grasslands and shrubs (21%) and croplands (11%). The original methane emissions rates (nmolCH_4 m^{-2} s^{-1}) were then integrated to give daily estimates of methane emissions (μmolCH_4 m^{-2} d^{-1}).

The daily rates of methane emission were then standardized to 15 °C to provide comparable estimates of methane emission capacities between sites using the Boltzmann–Arrhenius relationship:

$$\ln[\text{ME}_i(T)] = E_{\text{ME}}\left(\frac{1}{k_{\text{B}}\,T_{15}} - \frac{1}{k_{\text{B}}\,T_i}\right) + \ln[\text{ME}(T_{15})] \quad (3)$$

where $\ln[\text{ME}_i(T)]$ is the natural-logarithm-transformed rate of daily methane emissions by any site i ($i = 1, 2, \ldots 19$) under air temperature T in Kelvin, and

$\left(\frac{1}{k_B T_{15}} - \frac{1}{k_B T_i}\right)$ is the standardized temperature for site i. T_{15} (15 °C equals 288.15 K) is the temperature used to centre the temperature data. Therefore, the slope term E_{ME} represents the temperature sensitivity, and the intercept $\ln[ME(T_{15})]$ is the estimated daily capacity of methane emission standardized to 15 °C. The values of $\ln[ME(T_{15})]$ were then modelled as a simple linear function of annual average site temperatures using the lm function.

Temperature sensitivity and capacity of methane production and oxidation. We estimated the temperature sensitivity and capacity of methane production and oxidation using the Boltzmann–Arrhenius equation[7]:

$$\ln[F_{ij}(T)] = (\bar{E} + a_i + a_j)\left(\frac{1}{k_B T_C} - \frac{1}{k_B T_{ij}}\right) + \left(\overline{\ln[F(T_C)]} + b_i + b_j\right) \quad (4)$$

where $F_{ij}(T)$ is the rate of methane production or oxidation by sediment from pond i ($i = 1, 2, \ldots$), collected in month j ($j = 1, 2, \ldots$). As our experimental design yielded replicate responses in ponds for both treatments over months, we treated the sampling month and replicate pond as crossed random effects on the slope ($a_i + a_j$) and the intercept ($b_i + b_j$) of the models to account for the random variation among months and ponds from the fixed effect. The methane oxidation experiments were performed in only three months; therefore, the parameter 'sampling month' was not included to improve model convergence. The slope $\bar{E}$ of equation (4) represents the estimated population activation energy (temperature sensitivity) in units of eV, for either methane production ($\overline{E_{MP}}$) or oxidation ($\overline{E_{MO}}$). We standardized the plot using the term $\frac{1}{k_B T_C}$, in which T_C (288.15 K) is the average temperature in the ambient ponds (that is, 15 °C in 2017) and k_B is the Boltzman constant, so that the term $\overline{\ln[F(T_C)]}$ corresponds to the average capacity of methane production or oxidation at T_C. The effects of treatment (that is, ambient or warmed ponds) and substrates on methane production, on both the slope (the temperature sensitivity) and intercept (the average capacity of methane production or oxidation at T_C), were modelled as fixed effects.

The data were fitted into linear mixed-effect models using the lme4 package[41]. The details of model fitting, selection and validation are provided in Supplementary Tables 7 and 9 for production and oxidation, respectively. After the best-fitting model was determined, post hoc pairwise comparisons of the estimated marginal means of methane production capacity and temperature sensitivity were obtained using the emmeans package[42].

Turnover decay constants for organic carbon. We derived turnover decay constants k (h^{-1}) as a relative indicator of sediment carbon quality[43]:

$$k = \frac{R}{C} \quad (5)$$

where R is the rate of CO_2 production standardized to 15 °C (nmol g^{-1} h^{-1}) in anoxic slurry incubations, and C is the concentration of organic carbon (nmol g^{-1}). To characterize the proportion of organic carbon converted to methane in the sediments, we fitted k as an explanatory variable into a mixed-effect model:

$$\ln(MG_j) = (\text{slope} + a_j) \times \ln(k) + (\text{intercept} + b_j) \quad (6)$$

where $\ln(MG_j)$ is the natural logarithm of methane production capacity standardized to 15 °C by any sediment collected in month j. The slope represents the potential to produce methane in response to carbon quality, and the intercept represents the proportion of organic carbon converted to methane (that is, methane produced per unit carbon turned over). The random effect terms a_j and b_j represent variation among sampling months. The effects of treatment (that is, warmed or ambient) on the intercept and slope were fitted into the model as a fixed effect, and its significance was tested using the LRT (Supplementary Table 8).

Kinetic concentration effect on rates of methane oxidation. The kinetic concentration effect on rates of CH_4 oxidation was characterized using a Michaelis–Menten model:

$$MO_i(C_{CH_4}) = \frac{(V_{max} + a_i) \times C_{CH_4}}{(K_M + b_i) + C_{CH_4}} \quad (7)$$

where MO_i is the rate of ^{13}C-CH_4 oxidation by any sediment of pond i, and C_{CH_4} is the initial ^{13}C-CH_4 concentration. The parameters V_{max} and K_M, referring to the maximum rate and the concentration of methane at half V_{max}, respectively, were determined by fitting self-starting nonlinear mixed-effect models. The mesocosm ponds were fitted into the models as random effects to account for their variations on the parameter V_{max} (a_i) and on the parameter K_M (b_i), and the significance of warmed or ambient ponds was tested using the LRT (Supplementary Table 9).

CCE of methanotrophy. To characterize temperature and kinetic effects on the CCE, we fitted CCE as a response variable into a mixed-effect model:

$$CCE_i(T) = (\text{slope} + a_i) \times (T - T_C) + \left(\overline{CCE(T_C)} + b_i\right) \quad (8)$$

$$CCE_i(C_{CH_4}) = (\text{slope} + a_i) \times C_{CH_4} + \left(\overline{CCE(C_{CH_4,0})} + b_i\right) \quad (9)$$

where $CCE_i(T)$ and $CCE_i(C_{CH_4})$ are the CCE (%) by any sediment from pond i at temperature T or with an initial concentration of ^{13}C-CH_4 C_{CH_4}. To quantify the temperature sensitivity, we centred the plot to the average annual temperature in the ambient ponds (15 °C), so that the term $\overline{CCE(T_C)}$ represents the average CCE at 15 °C. However, we did not centre equation (9), and the intercept term $\overline{CCE_i(C_{CH_4,0})}$ is the CCE estimate at 0 μmol l^{-1}. The random effect terms a_i and b_i represent variation among ponds, and the effects of warmed or ambient ponds on the intercept and slope were fitted and tested as above (Supplementary Table 10).

Microbial community analysis. *Sediment sampling and DNA extraction.* Monthly sediment samples were collected from March 2016 to August 2017 from eight warmed and eight ambient ponds using cut-off 25 ml syringes. The top 2 cm of sediment was transferred into an Eppendorf tube and the rest into a Falcon tube and stored at −80 °C. DNA was extracted from 0.5 g of wet sediment (DNeasy PowerSoil Kit, Qiagen), and the DNA yield was quantified using NanoDrop (Thermo Scientific) according to the manufacturer's instructions. The yield was 1–4 μg per g wet sediment.

PCR amplification and sequencing. The *mcrA* gene, a molecular marker for methanogens, was amplified using mcrIRD primers[44] (forward, 5′-TWYGACCARATMTGGYT-3′; reverse, 5′-ACRTTCATBGCRTARTT-3′). PCRs were performed in 50 μl containing 25 μl of MyTaq Red Mix (Bioline), 1 μl of each primer (10 μM), 3 μl of DNA template and 20 μl of molecular biology quality water. The amplifications were performed in a T100 Cycler (Bio-Rad) following the thermal program: (1) 95 °C for 5 min; (2) 40 cycles at 95 °C for 45 s, 51 °C for 45 s and 72 °C for 60 s; (3) 72 °C for 5 min.

The *pmoA* gene, a molecular marker for methanotrophs, was amplified using a seminested PCR with A189F (5′-GGNGACTGGGACTTCTGG-3′)–A682R(5′-GAASGCNGAGAAGAASGC-3′) in the first round and A189F (5′-GGNGACTGGGACTTCTGG-3′)–A650R (5′-ACGTCCTTACCGAAGGT-3′) in the second round[45]. PCRs were performed in 25 μl containing 12.5 μl of MyTaq Red Mix (Bioline), 1 μl of each primer (10 μM), 1 μl of DNA and 9.5 μl of molecular biology quality water. For the first round, a touch-down PCR (ref. [45]) was performed in a T100TM Cycler (Bio-Rad) following the thermal program: (1) 94 °C for 3 min; (2) 30 cycles at 94 °C for 45 s, 62 to 52 °C for 60 s (initially decreasing by 0.5 °C per cycle down to 52 °C) and 72 °C for 180 s; (3) 72 °C for 10 min. The second round followed the thermal program: (1) 94 °C for 3 min; (2) 22 cycles at 94 °C for 45 s, 56 °C for 60 s and 72 °C for 60 s; (3) 72 °C for 10 min. The PCR products were checked by agarose gel electrophoresis and stained with GelRed.

Before sequencing, the PCR products were cleaned using Agencourt AMPure XP beads (Beckman Coulter). Barcodes and linkers were added by a ten-cycle PCR (95 °C for 3 min; 10 cycles of 98 °C for 20 s, 55 °C for 15 s and 72 °C for 15 s; 72 °C and 5 min). The final PCR products were quantified with a Qubit 2.0 Fluorometer (Invitrogen). 250 ng of PCR product from each sample was normalized to 4 nmol (SequalPrep Normalization Plate Kit, Invitrogen) and combined for sequencing on the Illumina MiSeq platform (300 base-pair paired-end) at the Genomics Service, University of Warwick.

Processing of sequence data. The downstream sequence analysis was conducted using QIIME2 (v.2018.2.0)[46] on the Apocrita HPC facility at Queen Mary University of London, supported by QMUL Research-IT (ref. [47]). Paired-end de-multiplexed files were imported into QIIME2 and processed using DADA2 for modelling and correcting amplicon errors[48]. The primer sequences were trimmed; low-quality sequences (quality score < 35) and chimaeras were removed. Amplicon sequence variants were then inferred by DADA2. To analyse the data at the genus level, amplicon sequence variants were clustered first into species-level OTUs at 85% similarity for *mcrA* and 90% for *pmoA* sequences[49,50]. OTUs were named using the pretrained Naïve Bayes classifier using custom databases[51,52] to specific genus-level clusters (Supplementary Tables 4 and 5). The classifier was trained on sequences extracted for the appropriate *mcrA* and *pmoA* gene fragments.

One *mcrA* sample was not analysed as it contained too few sequence reads. The final dataset contained 68 unique *mcrA* OTUs from 1,633,993 reads and 65 unique *pmoA* OTUs from 2,013,666 reads.

Phylogenetic analysis. The classified sequence data was further analysed using phyloseq in R (ref. [53]).

Variation in richness (α-diversity). For each sample, OTU richness, Chao1 index, Shannon's diversity index and evenness were calculated. The differences between treatments were determined using mixed-effect models, fitting each experimental pond as a random effect. To test the significance of long-term warming on α-diversity, an LRT was performed comparing full and reduced models (Supplementary Figs. 2 and 5).

Variation in community composition (β-diversity). PCoA was used to analyse the communities between treatments using a Bray–Curtis dissimilarity index with Hellinger standardized datasets at the genus level. The scores of the samples along the PCoA axes, with the two largest eigenvalues, were fitted into mixed-effect models, and the significance of long-term warming on the scores was tested as above[41]

(Supplementary Table 3). PERMANOVA (ref. [54]) with the adonis function (vegan package)[55] was used to partition variation in a distance matrix between treatments using a permutation test with pseudo-*F* ratios with similar results to the PCoA.

Differences in taxonomic abundance. Changes in abundance under warming were investigated using a negative binomial generalized linear model using DESeq2 (ref. [56]). DESeq2 was designed for RNA-seq data but has been used to analyse microbiome data[56], especially if the libraries are evenly sized. Change under warming at the genus level was estimated by setting the false discovery rate to 0.01.

Quantitative PCR of methanogens and methanotrophs. Methanogen and methanotroph population sizes in sediment DNA samples were determined using qPCR with the mcrIRD primers (*mcrA*) and A189F–A650 primers (*pmoA*), respectively. Amplifications were performed using CFX384 Touch Real-Time PCR (Bio-Rad) in a total volume of 10 µl containing 5 µl of SsoAdvanced Universal SYBR Green Supermix (Bio-Rad), 0.2 µl of each primer (10 µM), 1 µl of DNA template and 3.6 µl of molecular biology quality water. Standard curves (10^2–10^7 copies per µl) were constructed by serial diluting plasmid DNA containing *mcrA* or *pmoA* gene inserts.

The qPCR program for *mcrA* was: (1) 98 °C for 3 min; (2) 40 cycles at 98 °C for 15 s, 55 °C for 15 s and 72 °C for 60 s; (3) 95 °C for 10 s. The qPCR program for *pmoA* was: (1) 96 °C for 5 min; (2) 40 cycles at 94 °C for 45 s, 60 °C for 45 s and 72 °C for 45 s. The specificity and size of the products were confirmed by melt curve analysis after the final extension.

Cell-specific activities of methanogens and methanotrophs. Cell-specific activities were calculated for both methanogens and methanotrophs by dividing CH_4 production and oxidation capacity at 15 °C by the *mcrA* and *pmoA* gene copy abundances, respectively.

Reporting Summary. Further information on research design is available in the Nature Research Reporting Summary linked to this article.

Data availability

The data that support the findings of this study are available from the corresponding author upon request. The DNA sequences are in the National Center for Biotechnology Information database, under BioProject ID PRJNA484117. Source data are provided with this paper.

References

37. Yver Kwok, C. E. et al. Methane emission estimates using chamber and tracer release experiments for a municipal waste water treatment plant. *Atmos. Meas. Tech.* **8**, 2853–2867 (2015).
38. Sanders, I. A. et al. Emission of methane from chalk streams has potential implications for agricultural practices. *Freshw. Biol.* **52**, 1176–1186 (2007).
39. Neubacher, E. C., Parker, R. E. & Trimmer, M. Short-term hypoxia alters the balance of the nitrogen cycle in coastal sediments. *Limnol. Oceanogr.* **56**, 651–665 (2011).
40. R: a language and environment for statistical computing v.3.2.5 (R Core Team, 2014).
41. Kuznetsova, A., Brockhoff, P. B. & Christensen, R. H. B. {lmerTest} package: tests in linear mixed effects models. *J. Stat. Softw.* **82**, 1–26 (2017).
42. Lenth, R. emmeans: estimated marginal means, aka least-squares means. R package v.1.4.7 (2019); https://cran.r-project.org/package=emmeans
43. Nicholls, J. C. & Trimmer, M. Widespread occurrence of the anammox reaction in estuarine sediments. *Aquat. Microb. Ecol.* **55**, 105–113 (2009).
44. Lever, M. A. & Teske, A. P. Diversity of methane-cycling archaea in hydrothermal sediment investigated by general and group-specific PCR primers. *Appl. Environ. Microbiol.* **81**, 1426–1441 (2015).
45. Horz, H. P., Rich, V., Avrahami, S. & Bohannan, B. J. M. Methane-oxidizing bacteria in a California upland grassland soil: diversity and response to simulated global change. *Appl. Environ. Microbiol.* **71**, 2642–2652 (2005).
46. Caporaso, J. G. et al. QIIME allows analysis of high-throughput community sequencing data. *Nat. Methods* **7**, 335–336 (2010).
47. King, T., Butcher, S. & Zalewski, L. *Apocrita—High Performance Computing Cluster for Queen Mary University of London* (Queen Mary University of London, 2017); https://doi.org/10.5281/ZENODO.438045
48. Callahan, B. J. et al. DADA2: high-resolution sample inference from Illumina amplicon data. *Nat. Methods* **13**, 581–583 (2016).
49. Pester, M., Friedrich, M. W., Schink, B. & Brune, A. *pmoA*-based analysis of methanotrophs in a littoral lake sediment reveals a diverse and stable community in a dynamic environment. *Appl. Environ. Microbiol.* **70**, 3138–3142 (2004).
50. Oakley, B. B., Carbonero, F., Dowd, S. E., Hawkins, R. J. & Purdy, K. J. Contrasting patterns of niche partitioning between two anaerobic terminal oxidizers of organic matter. *ISME J.* **6**, 905–914 (2012).
51. Wilkins, D., Lu, X. Y., Shen, Z., Chen, J. & Lee, P. K. H. Pyrosequencing of *mcrA* and archaeal 16s rRNA genes reveals diversity and substrate preferences of methanogen communities in anaerobic digesters. *Appl. Environ. Microbiol.* **81**, 604–613 (2015).
52. Yang, S., Wen, X. & Liebner, S. *pmoA Gene Reference Database (Fasta-Formatted Sequences and Taxonomy)* (GFZ Data Services, 2016).
53. McMurdie, P. J. & Holmes, S. phyloseq: an R package for reproducible interactive analysis and graphics of microbiome census data. *PLoS ONE* **8**, e61217 (2013).
54. Anderson, M. J. in *Wiley StatsRef: Statistics Reference Online* 1–15 (Wiley, 2017).
55. Oksanen, J. et al. vegan: community ecology package. R package v.2.5-6 (2018); https://cran.r-project.org/package=vegan
56. Love, M. I., Huber, W. & Anders, S. Moderated estimation of fold change and dispersion for RNA-seq data with DESeq2. *Genome Biol.* **15**, 550 (2014).

Acknowledgements

This study was supported by Queen Mary University of London and the UK Natural Environment Research Council (grant nos NE/M02086X/1 and NE/M020886/1). We thank I. Sanders and F. Shelley for technical and fieldwork assistance, J. Pretty for mesocosm pond maintenance, M. Rouen for designing and installing the Campbell control and data-logging system, H. Prentice for collecting sediments and for DNA extraction, C. Economou and M. Struebig for help with the molecular work, and P. K. H. Lee for providing the *mcrA* database and related documents for the bioinformatics analysis. We thank the principal investigators of the methane flux data products, including W. Quinton, O. Sonnentag, G. Wohlfahrt, S. Gogo, T. Schuur, K. Krauss, A. Desai, G. Bohrer, R. Vargas, D. Baldocchi, J. Chen, H. Chu, H. Iwata, M. Ueyama and Y. Harazono. We also thank the funding agencies that supported their flux measurements.

Author contributions

M.T., Y.Z. and K.J.P conceived the study. Y.Z. conducted the vast majority of the experiments and analysed the data. Y.Z., M.T., K.J.P., G.Y.-D. and A.J.D. discussed the data. Y.Z., M.T. and K.J.P. wrote the manuscript, and all authors contributed to revisions. Y.Z. and S.F.H. set up the chamber system. Y.Z., O.E. and L.S. performed the molecular analyses.

Competing interests

The authors declare no competing interests.

Additional information

Extended data is available for this paper at https://doi.org/10.1038/s41558-020-0824-y.

Supplementary information is available for this paper at https://doi.org/10.1038/s41558-020-0824-y.

Correspondence and requests for materials should be addressed to M.T.

Reprints and permissions information is available at www.nature.com/reprints.

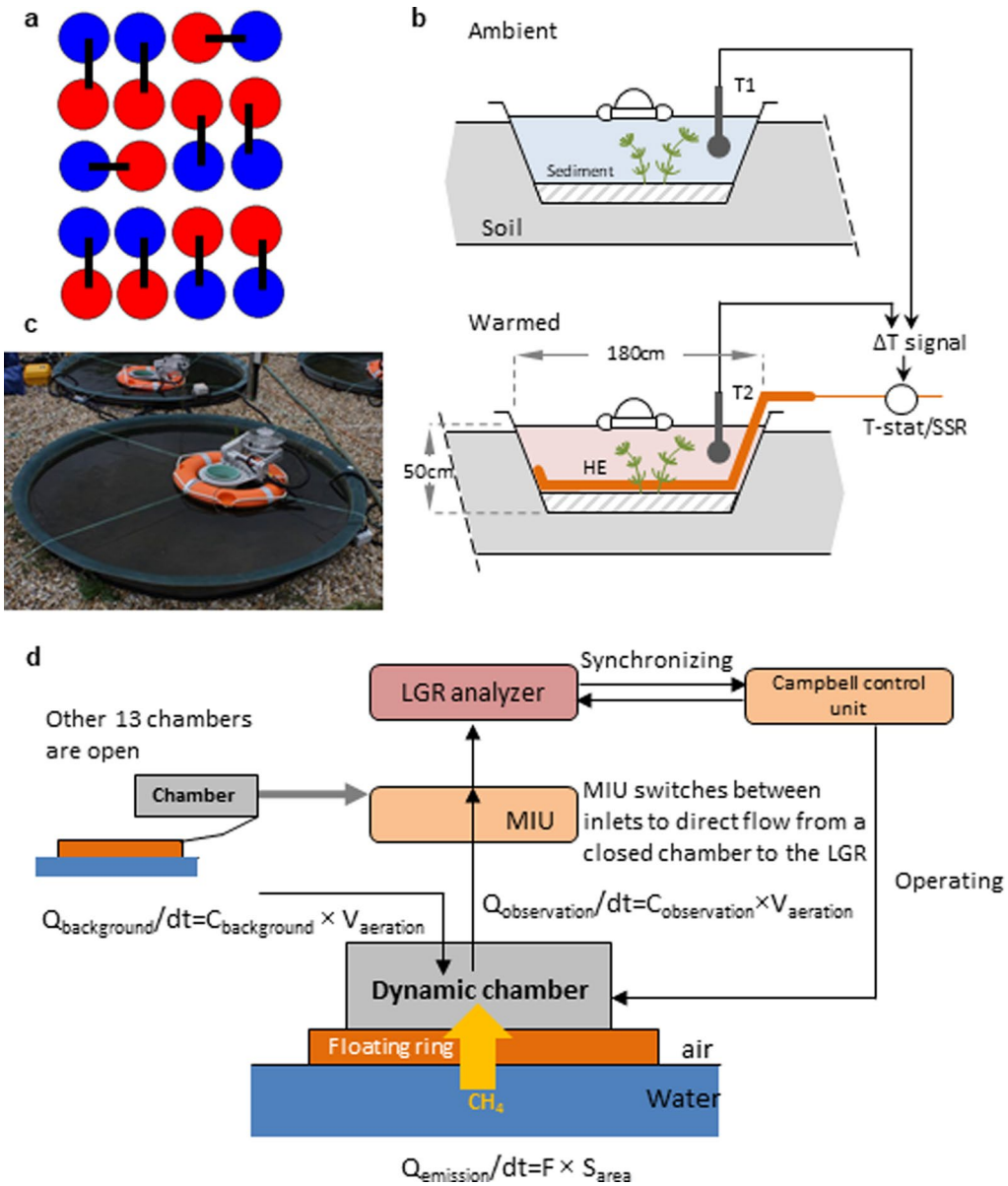

Extended Data Fig. 1 | Schematic of experimental pond set-up and dynamic chamber measurements. Twenty artificial ponds, with 10 warmed (red) by 4 °C above 10 ambient (blue) ponds, were paired in a randomized block design (**a**) and controlled via two temperature sensors (T1, T2), a thermocouple (T-stat) and a solid-state relay (SSR) (**b**). Dynamic LI-COR chambers, floating on lifebuoys, were installed on 7 each of the warmed and ambient ponds (**c**). Each floating chamber was connected to one of the inlet ports on the MIU and the MIU outlet port was connected to the gas inlet port of Ultra-Portable Greenhouse Gas Analyzer (LGR) (**d**). A dynamic chamber is sequentially triggered to close by a customised Campbell control unit (CCU) for 30 minutes for gas measurements while the other chambers remain open. When a chamber is triggered to close, the MIU switches simultaneously to the inlet connected to the closing chamber to direct its gas flow to the LGR. *See* Methods and Extended Data Fig. 2 for further details on methane emissions.

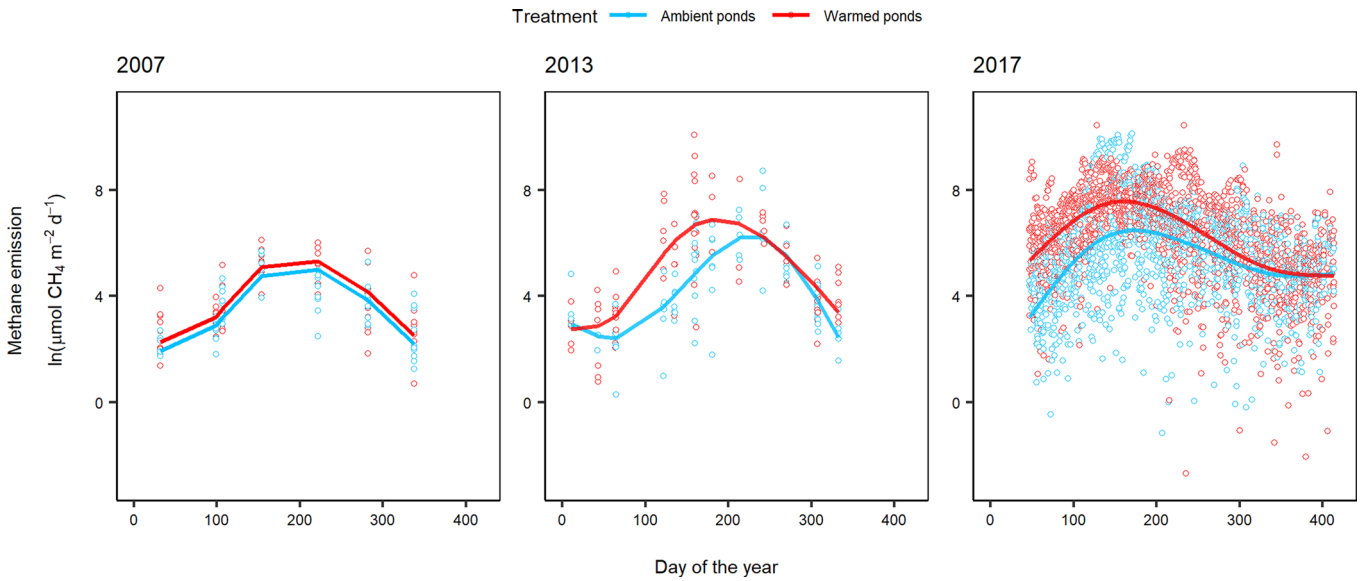

Extended Data Fig. 2 | Consistent seasonal patterns in daily methane emissions under warming but with ongoing divergence over 10 years (2007[35], 2013[20] and 2017 (this study)). The seasonal patterns in all 3 years are very similar, despite the use of different techniques but the frequent measurements (three times daily) using dynamic chambers in 2017 captured far more details in emissions compared to 2007 and 2013 when static chambers were used to measure methane emission on 7 and 12 occasions over each year, respectively. Note the natural log scale for methane emissions.

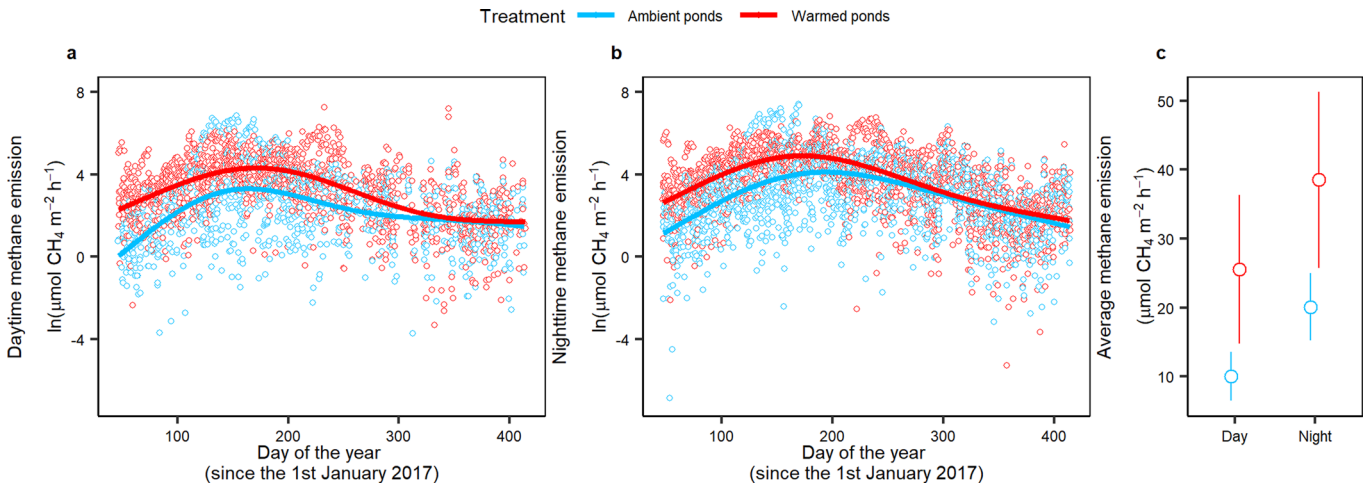

Extended Data Fig. 3 | Methane emissions at night and during the day. Methane emissions during the day (**a**) and at night (**b**) follow similar seasonal patterns; yet methane emissions at night are significantly greater than during the day (**c**).

nature research

Corresponding author(s): Mark Trimmer

Last updated by author(s): 25/04/20

Reporting Summary

Nature Research wishes to improve the reproducibility of the work that we publish. This form provides structure for consistency and transparency in reporting. For further information on Nature Research policies, see Authors & Referees and the Editorial Policy Checklist.

Statistics

For all statistical analyses, confirm that the following items are present in the figure legend, table legend, main text, or Methods section.

n/a	Confirmed	
☐	☒	The exact sample size (*n*) for each experimental group/condition, given as a discrete number and unit of measurement
☐	☒	A statement on whether measurements were taken from distinct samples or whether the same sample was measured repeatedly
☐	☒	The statistical test(s) used AND whether they are one- or two-sided *Only common tests should be described solely by name; describe more complex techniques in the Methods section.*
☒	☐	A description of all covariates tested
☒	☐	A description of any assumptions or corrections, such as tests of normality and adjustment for multiple comparisons
☐	☒	A full description of the statistical parameters including central tendency (e.g. means) or other basic estimates (e.g. regression coefficient) AND variation (e.g. standard deviation) or associated estimates of uncertainty (e.g. confidence intervals)
☐	☒	For null hypothesis testing, the test statistic (e.g. *F*, *t*, *r*) with confidence intervals, effect sizes, degrees of freedom and *P* value noted *Give P values as exact values whenever suitable.*
☒	☐	For Bayesian analysis, information on the choice of priors and Markov chain Monte Carlo settings
☒	☐	For hierarchical and complex designs, identification of the appropriate level for tests and full reporting of outcomes
☒	☐	Estimates of effect sizes (e.g. Cohen's *d*, Pearson's *r*), indicating how they were calculated

Our web collection on statistics for biologists contains articles on many of the points above.

Software and code

Policy information about availability of computer code

Data collection	Methane and carbon dioxide emission data were collected using Ultra-Portable Greenhouse Gas Analyzer software. Quantitative PCR data was collected using Bio-Rad CFX Manager (version 3.1).
Data analysis	Sequence analysis was conducted using QIIME2 (version 2018.2.0) and statistical analysis was performed in R (version 3.4.4)

For manuscripts utilizing custom algorithms or software that are central to the research but not yet described in published literature, software must be made available to editors/reviewers. We strongly encourage code deposition in a community repository (e.g. GitHub). See the Nature Research guidelines for submitting code & software for further information.

Data

Policy information about availability of data

All manuscripts must include a data availability statement. This statement should provide the following information, where applicable:

- Accession codes, unique identifiers, or web links for publicly available datasets
- A list of figures that have associated raw data
- A description of any restrictions on data availability

The DNA sequences reported in this study were available through the National Center for Biotechnology Information database, under the BioProject ID PRJNA484117. The authors declare that all data supporting the findings of this study are available from the corresponding author upon request.

Field-specific reporting

Please select the one below that is the best fit for your research. If you are not sure, read the appropriate sections before making your selection.

☐ Life sciences ☐ Behavioural & social sciences ☒ Ecological, evolutionary & environmental sciences

For a reference copy of the document with all sections, see nature.com/documents/nr-reporting-summary-flat.pdf

Ecological, evolutionary & environmental sciences study design

All studies must disclose on these points even when the disclosure is negative.

Study description	Using a well-replicated (n=20), long-term (since 2006) freshwater warming experiment (+4ºC above ambient), we investigated how the ecosystem-level methane cycle and methane-related microorganisms would be altered by warming (see Methods for description for pond facility). Methane and carbon dioxide emissions were first measured three times daily over the annual cycle in 2017 using an Ultra-Portable Greenhouse Gas Analyzer (LGR) and multiplexed automatic open chamber systems from seven ambient and seven warmed replicate ponds. Chambers were closed for 30 minutes to measure gases at steady-state and LGR switches between each chamber automatically. To investigate the methane production capacity, sediments cores were collected by hand using small cores (Ø 34 mm) every month from January, 2016, to December, 2016, (except for July) from three to five warmed and and three to five ambient ponds assigned randomly to the 10 ponds in each treatment. Additional substrates, i.e., acetate and hydrogen, were added to a final concentrations at 10 mM (or 17 % for hydrogen) to the same sediments to investigate the effect of long-term warming on methanogenic pathways. In May, June and July, 2017, sediment cores were collected form eight warmed and eight ambient ponds using trunctated 25 ml syringes to measure the temperature sensitivity and capacity of methane oxidation. In December, 2018, more sediment cores from the same ponds using the same techniques were collected to investigate the kinetic concentration effect on methane oxidation rate. In order to characterize the microbial community composition and functional gene abundance, the sediment samples were collected every month from March to August in 2016 and 2017 from eight warmed and eight ambient ponds using cut-off 25 ml syringes. The sediments from the top 2 cm were used for methanotroph community analyses while the rest was used for methanogen community analyses. The mcrA gene and pmoA gene were used as molecular markers for community composition and abundance for methanogen and methanotroph, respectively.
Research sample	Our well replicated (n=20) freshwater mesocsom ponds were designed to mimic shallow lakes and have previously been reported on between 2010 to 2017. The mesocosm ponds provide a good representation of freshwater ecosystems under warming scenarios as the disproportionate increase in methane emissions induced by long-term warming maps onto a trend of methane emissions, in a meta-analysis, from naturally warmer ecosystems. The methane emission in the meta-analysis were downloaded within the AmeriFLux network and the EuroFlux network.
Sampling strategy	The methane emissions were measured three times daily during an annual cycle to measure the annual average of methane emissions. The methane production samples were collected monthly in 2016 to guarantee a representative overall estimates. The methane oxidation samples were collected in fewer months but more ponds were sampled to improve the overall estimates.
Data collection	The methane and carbon dioxide emission data were collected by Ultra-Portable Greenhouse Gas Analyzer and its computer software. The data were collected by Yizhu Zhu. The sediment corers for methane production and oxidation experiments were collected by Yizhu Zhu. The sediment samples for microbial community analyses were collected by Yizhu Zhu and Hannah Prentice. The lab experiments were performed by Yizhu Zhu.
Timing and spatial scale	The methane emission measurements were acquired at 1 Hz 24 hours during annual cycle from February, 2017 to February, 2018. For methane production and oxidation capacity, the sediment corers were collected in afternoon (1 pm to 3 pm). The methane production was quantified every 24 hours and the incubation lasted for up to 4 days. In the kinetic methane concentrations on methane oxidation rate experiment, the samples with less than 15 µmol per L 13C-CH4 were incubated for less than 12 hours while those with higher methane concentrations were incubated overnight for ~20 hours. In the temperature sensitivity and capacity of methane oxidation experiment, all samples were incubated overnight for ~20 hours.
Data exclusions	Ebullition events (1.2%) were characterized and excluded to allow for calculating CH4 emissions at steady-state (see Methods). The rate of CH4 production plateaued in the incubation above 22 °C and were therefore excluded from the statistical analysis. The outliers beyond the 95th percentiles were removed from the ratio of CH4 to CO2 emission analysis. One mcrA sequencing sample was not analyzed as it contained <5,000 sequence reads.
Reproducibility	The experimental ponds were well replicated (n=20). The methane and carbon dioxide emission were measured three times daily during an annual period to guarantee reproducibility. The sediments in methane production experiment were collected monthly for eleven months in 2016 from 3 to 5 ambient and 3 to 5 warmed ponds, randomly selected, to improve the overall estimates of methane production capacity in the sediments. In methane oxidation experiment, sediments cores were collected from 16 ponds (8 ambient and 8 warmed ponds) to improve the overall estimates. For community analyses, the sediment samples were collected in five months from 16 ponds (8 ambient and 8 warmed ponds) to guarantee a representative result.
Randomization	The ponds were randomly selected for sampling.
Blinding	Yizhu Zhu collected and processed the samples and blinding was not possible or appropriate.

Did the study involve field work? ☐ Yes ☒ No

Reporting for specific materials, systems and methods

We require information from authors about some types of materials, experimental systems and methods used in many studies. Here, indicate whether each material, system or method listed is relevant to your study. If you are not sure if a list item applies to your research, read the appropriate section before selecting a response.

Materials & experimental systems

n/a	Involved in the study
☒	☐ Antibodies
☒	☐ Eukaryotic cell lines
☒	☐ Palaeontology
☐	☒ Animals and other organisms
☒	☐ Human research participants
☒	☐ Clinical data

Methods

n/a	Involved in the study
☒	☐ ChIP-seq
☒	☐ Flow cytometry
☒	☐ MRI-based neuroimaging

Animals and other organisms

Policy information about studies involving animals; ARRIVE guidelines recommended for reporting animal research

Laboratory animals	No laboratory animals we involved in this study.
Wild animals	No wild animals were involved in this study.
Field-collected samples	The experimental mesocosm ponds are located outside at the Freshwater Biological Laboratory in Dorset but we do not consider their routine sampling as fieldwork. We do, however, keep all collected samples in a cool box during transport to the laboratory in London.
Ethics oversight	No ethical approval was required for this study.

Note that full information on the approval of the study protocol must also be provided in the manuscript.